© 2017. Published by The Company of Biologists Ltd | Development (2017) 144, 4637-4644 doi:10.1242/dev.152827

RESEARCH ARTICLE

Juvenile hormone signaling in short germ-band hemimetabolan embryos

Ana Fernandez-Nicolas and Xavier Belles*

ABSTRACT

The role of juvenile hormone (JH) in insect embryos is far from understood, especially in short germ-band hemimetabolan species. To shed light on this issue, we depleted the mRNA levels of Krüppel homolog 1, Methoprene-tolerant and JH acid *O*-methyltransferase, key elements of JH signaling, in embryos of the short germ-band hemimetabolan species *Blattella germanica*. This precluded the formation of the germ-band anlage in a group of embryos. Hatchability was also reduced, which might have been caused by premature upregulation of laccase 2, a promoter of cuticle tanning. In other cases, development was interrupted in mid embryogenesis, involving defects related to dorsal closure and appendage formation. These phenotypes possibly result from the low levels of Broad-complex (BR-C) produced under JH-depleted conditions. This contrasts with holometabolan species, in which JH does not promote *BR-C* expression, which remains low during embryo development. Possibly, the stimulatory role of JH on *BR-C* expression and the morphogenetic functions of BR-C in hemimetabolan embryos were lost in holometabolan species. If so, this might have been a key driver for the evolution of holometabolan metamorphosis.

KEY WORDS: Juvenile hormone, Krüppel homolog 1, Methoprene-tolerant, Juvenile hormone acid *O*-methyltransferase, Broad complex, *Blattella*

INTRODUCTION

Does juvenile hormone (JH) signaling play a role in embryo development in insects? The question is of interest because it has been suggested that embryonic JH could be a determining factor in hemimetabolan or holometabolan metamorphosis (Truman and Riddiford, 1999), whereas recent studies indicate that it only has rather accessory roles, if any, at least in holometabolan species (Daimon et al., 2015).

The evolution of metamorphosis has been explained on the basis of a heterochrony; hemimetabolan species develop the basic adult body plan during embryogenesis, whereas holometabolan species delay adult body plan construction until the pupal stage (Belles, 2011; Truman and Riddiford, 1999). Heterochrony is an interesting concept but the underlying mechanisms are far from understood. In this context, Truman and Riddiford proposed that embryonic JH might be an important factor in the evolutionary shift from hemimetaboly to holometaboly after noticing that the hormone is produced earlier in holometabolan embryogenesis (Truman and Riddiford, 1999, 2002). Thus, the premature production of JH might have precluded the formation of the adult body plan in holometabolan embryos. Previous studies had shown that treating embryos with JH often results in a variety of developmental defects in ametabolan (Rohdendorf and Sehnal, 1973), hemimetabolan (Enslee and Riddiford, 1977) and holometabolan species (Matolín and Gelbic, 1975; Smith and Arking, 1975). A subsequent and careful study based on the hemimetabolan species *Acheta domesticus* showed that eggs treated with JH during early embryogenesis resulted in a premature formation of nymphal-like bristle patterning and sclerotized mandibles (Erezyilmaz et al., 2004). Intriguingly, this might suggest that JH is involved in the formation of the nymph in mid to late embryogenesis.

However, JH treatments cannot reveal the precise role of embryonic JH. Indeed, suppression of JH signaling would be a better approach for unveiling this possible role. The first experiments conducted along this line involved treating embryos with precocenes, compounds that destroy the corpora allata (CA), the JH-producing glands. One of the most robust studies was performed on the locust *Locusta migratoria* as the authors assessed that precocene treatment had destroyed the embryo CA (Aboulafia-Baginsky et al., 1984). The eggs in late stages of embryogenesis (when JH is being produced by the CA) treated with precocene either did not hatch (39%) or died in the first or second nymphal instar. Precocenes are highly selective for CA cells but can also act on other tissues (Pratt et al., 1980). Therefore, a more suitable approach would be to generate knockout insects with null mutations in genes critical for JH biosynthesis or transduction. This was the approach followed in the silkworm *Bombyx mori* by Daimon et al. (2015), who used a genome-editing tool such as TALENs (targeted mutagenesis mediated by transcription activator-like effector nucleases). Using TALENs, Daimon and colleagues suppressed the production of JH acid *O*-methyltransferase (JHAMT), an enzyme that catalyzes the final or penultimate step in JH biosynthesis, and the JH receptor Methoprene-tolerant (Met). Surprisingly, their results suggested that JH has no relevant roles in *B. mori* embryogenesis as only hatchability was affected in JHAMT mutants, with the day of hatching delayed by a few days (Daimon et al., 2015).

The remarkable result obtained in *B. mori* led to the question of whether the practically dispensable role of JH in embryos is a general trend in insects or a peculiarity of the long germ-band, holometabolan species. To answer this question we studied the role of JH in embryos from a short germ-band hemimetabolan species, the cockroach *Blattella germanica*, and used the maternal RNA interference (RNAi) technique to knock down key members of the JH signaling pathway. Robust information is available about *B. germanica* embryo development (Konopová and Zrzavý, 2005; Piulachs et al., 2010), including the classification of embryogenesis in 18 well-defined stages (Tanaka, 1976), and precise JH and ecdysteroid measurements (Maestro et al., 2005, 2010). In addition,

Institute of Evolutionary Biology (CSIC-Universitat Pompeu Fabra), Passeig Marítim 37, 08003 Barcelona, Spain.

*Author for correspondence (xavier.belles@ibe.upf-csic.es)

X.B., 0000-0002-1566-303X

Received 29 March 2017; Accepted 13 October 2017

DEVELOPMENT

Development (2017) 144, 4637-4644 doi:10.1242/dev.152827

maternal RNAi depletes embryo transcripts efficiently in this cockroach (Piulachs et al., 2010). We chose the following interference targets from downstream to upstream of the signaling axis (Jindra et al., 2015a,b): Krüppel homolog 1 (*Kr-h1*), the main transducer of the JH signal during metamorphosis, *Met* and *JHAMT*. The three genes have been structurally and functionally characterized in *B. germanica* (Dominguez and Maestro, 2017; Lozano and Belles, 2011, 2014).

Our experiments showed that maternal RNAi for these three factors precluded the formation of the germ-band anlage in some cases, which led us to study the expression of a number of genes operating in early embryonic development. Therefore, we studied Mad, Smox and Medea; the Smads that are key signal transducers in transforming growth factor (TGF)-β pathways, and have relevant functions in insect embryogenesis, especially the bone morphogenetic protein (BMP) branch (Deignan et al., 2016). In *B. germanica*, the three Smads have been characterized in the context of metamorphosis (Santos et al., 2016). We also examined the expression of proliferating cell nuclear antigen (PCNA), a protein required for cell cycle progression and cellular proliferation (Kelman, 1997) that has been associated with nuclear division cycles in early insect embryogenesis (Yamaguchi et al., 1991). Additionally, we studied Zelda, a protein that plays an essential role in the activation of transcription from the earliest zygotic genes (Liang et al., 2008) by binding to specific sites in DNA and increasing chromatin accessibility (Schulz et al., 2015; Sun et al., 2015). Finally, we measured the expression of hunchback (*hb*), Krüppel (*Kr*) and orthodenticle (*otd*), which are gap genes involved in early embryonic patterning in short (*Tribolium castaneum*) and long germ-band insects (*Drosophila melanogaster*, *Nasonia vitripennis*) (Lynch et al., 2012).

Some of the embryos from treated females almost completed development, but showed an intensely sclerotized cuticle. This led us to examine the expression of laccase 2, a phenoloxidase involved in cuticle tanning (Arakane et al., 2005; Elias-Neto et al., 2010; Sugumaran and Barek, 2016). Laccase 2 expression was also measured in apparently normal nymphs that were unable to hatch resulting from the RNAi treatments, under the hypothesis that an altered expression of this gene could explain this phenotype.

RESULTS

Disrupting JH transduction: Kr-h1-depletion

The expression pattern of *Kr-h1* mRNA in the embryo is shown in Fig. 1A. The low, but well-measurable expression from the nonfertilized egg (NFE) stage to embryonic day (ED) 0 is intriguing as there is no detectable JH production in these very early stages (Maestro et al., 2010). The expression found from ED6 to ED16 coincided relatively precisely with the cycle of JH production by the embryonic CA (Maestro et al., 2010). This is consistent with the JH dependence of *Kr-h1* expression reported in nymphs (Lozano and Belles, 2011). In ED6, thus at the beginning of the embryonic JH cycle, transcript levels of *Kr-h1* were significantly lower in embryos from Kr-h1-depleted females compared with those from control females treated with dsMock. Subsequently, *Kr-h1* transcript levels were still significantly lower in embryos from treated females than in those from controls at ED9, but tended to be higher in embryos from treated females than in those from controls at ED13 (Fig. S1A).

Control females treated with dsMock (n=55) formed a normal ootheca on day 8 of adult life, which contained viable embryos that produced normal first instar nymphs 18 days later. Females treated with dsKr-h1 (n=70) also formed apparently normal oothecae on day 8, and 30 of them (42.9%) produced apparently well-formed first instar nymphs that eclosed normally on day 18, i.e. with no delay with respect to the controls. Twelve of these oothecae (17.1%) were dropped between days 2 and 3 (12-17% embryogenesis), five (7.1%) were dropped between days 7 and 15 (40-83% of embryogenesis), and 23 (32.9%) were transported beyond day 18

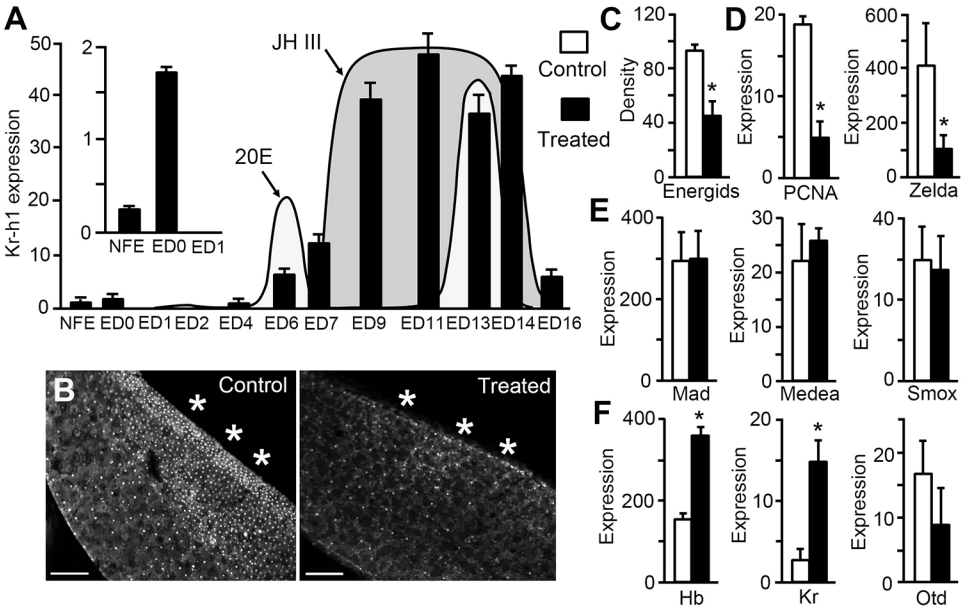

Fig. 1. Expression of Kr-h1 in embryos of *Blattella germanica* and effects of maternal RNAi on ED2. (A) *Kr-h1* mRNA levels in NFEs, and in embryos of different ages from ED0 to ED16; superimposed are the patterns of 20E and juvenile hormone III (JH III), according to the data of Maestro et al. (2005) and Maestro et al. (2010), respectively; the smaller chart shows the values in NFE, ED0 and ED1 on a larger scale. (B) Control and treated (Kr-h1-depleted) embryos showing the accumulation of energids in the ventral side (asterisks). Scale bars: 200 µm. (C) Density of energids (number of energids in 0.10 mm^2) in control and treated (Kr-h1-depleted) embryos. (D) Expression of PCNA and Zelda. (E) Expression of the Smads of the TGF-β pathways, Mad, Medea and Smox. (F) Expression of the gap genes *hb*, *Kr* and *otd*. Each measurement represents three biological replicates and results of qRT-PCR are expressed as copies of the examined transcript per 1000 copies of *BgActin-5c* mRNA. Data are presented as mean±s.e.m. *P<0.05 compared to controls, calculated on the basis of the relative expression software tool (REST) (Pfaffl et al., 2002).

Development (2017) 144, 4637-4644 doi:10.1242/dev.152827

without hatching (they spontaneously dropped from the female between days 19 and 21) (Table S1).

We were interested in studying the embryos of oothecae dropped between days 2 and 3, as they would inform about the functions of Kr-h1 in early embryos. ED2 controls were between stages 1 and 2 as defined by Tanaka (1976), showing a high density of energids, which accumulated on the ventral side of the egg, thus contributing to the formation of the germ-band anlage (Fig. 1B,C). We examined 252 embryos from the 12 oothecae produced by dsKr-h1-treated females that dropped between days 2 and 3. These embryos had interrupted development around the formation of the germ-band anlage, between Tanaka stages 1 and 2, and were thus comparable to ED2 controls. They showed fewer energids than the controls at the same age, and the germ-band anlage where the energids accumulate was thinner (Fig. 1B,C), although the energids cellularized, as in ED2 controls. PCNA and Zelda expression levels were lower in the Kr-h1-depleted embryos than in the controls (Fig. 1D), whereas the expression of the three Smads of the TGF-ß signaling pathway, Mad, Medea and Smox, was unaffected (Fig. 1E). Among the genes involved in early embryo patterning, the expression of *hb* and *Kr* was higher than in controls, whereas that of *otd* was unaffected (Fig. 1F).

At ED6, when *Kr-h1* mRNAs are effectively depleted (Fig. S1A), transcript levels of *Met* were unaffected whereas those of Broad-complex (*BR-C*) tended to be lower in embryos from Kr-h1-depleted females compared to controls (Fig. S1B). This suggests that BR-C expression is stimulated by JH in the embryo, being downstream of Kr-h1 in the JH signaling pathway. At ED6, PCNA expression levels still tended to be lower in Kr-h1-depleted embryos than in the controls (Fig. S1C), whereas Zelda expression had dramatically decreased in both groups (Fig. S1C). Mad, Medea and Smox expression was similar in Kr-h1-depleted and in control embryos (Fig. S1D), as in ED2 (Fig. 1E). *hb*, *Kr* and *otd* mRNA levels showed no significant differences between Kr-h1-depleted and control embryos (Fig. S1E).

Subsequently, we were interested in studying the embryos from the oothecae that were transported beyond day 18 without hatching. Thus, on day 19 we dissected 18 of these oothecae and then examined 452 of their embryos. In total, 176 of them (38.9%) had interrupted development around the formation of the germ-band anlage, between Tanaka stages 1 and 2 (phenotype A, Fig. 2A). A total of 102 embryos (22.6%) were segmented and had appendages, showing interrupted development between Tanaka stages 10 and 15, including diverse malformations, such as imperfectly sealed dorsal closure, a reduced abdomen or imperfect eyes (phenotype B, Fig. 2B). A total of 79 embryos (17.5%) were apparently well-formed nymphs, but featured an intensely sclerotized cuticle (phenotype C, Fig. 2C). Finally, 95 embryos (21.0%) were apparently well-formed nymphs but did not hatch (phenotype D, Fig. 2D). Phenotype D corresponds to nymphs practically indistinguishable from control prehatched nymphs, showing, for example, the typical nymphal microsculpture and chaetotaxy, and sclerotized mandibles. If the chorion was artificially broken, then most phenotype D specimens behaved as naturally eclosed first instar nymphs, with apparently normal morphology and motility (Fig. 2E) (see also Table S2). Phenotype A embryos resembled and appeared to correspond to those found in oothecae dropped between days 2 and 3. Most of the phenotype B embryos looked like some of the malformed embryos resulting from maternal RNAi of BR-C (Piulachs et al., 2010), which is not surprising as Kr-h1 depletion reduced BR-C expression (Fig. S1B). The intensely sclerotized nymphs of phenotype C were suggestive of an effect on cuticle tanning, thus we measured the expression of laccase 2 in these embryos, which was significantly higher than in controls (Fig. 2F). We also studied the expression of laccase 2 in phenotype D embryos, speculating that an altered expression of this gene might explain the problems of hatchability. Results showed that laccase 2 was significantly upregulated in phenotype D embryos (Fig. 2F) (see also Table S2).

Disrupting JH reception: Met depletion

Embryonic levels of *Met* mRNA are shown in Fig. 3A. Intriguingly, there is significant expression in early embryogenesis, especially at ED0 and ED1, and then a peak in expression on ED6, just before the onset of the JH production cycle. During this cycle, *Met* levels are quite constant, although comparatively low. Maternal RNAi reduced *Met* mRNA levels as shown by measurements at ED6 (Fig. S2A). At ED9, *Met* transcript levels were still significantly lower in treated embryos than in controls, but on ED13, *Met* transcript levels in both groups were similar (Fig. S2A).

On ED6, when *Met* mRNAs are effectively depleted (Fig. S2A), transcript levels of *Kr-h1* and *BR-C* were significantly reduced (Fig. S2B), which suggests that Kr-h1 and BR-C are downstream of Met in the JH signaling pathway in the embryo. At this age, PCNA and Zelda expression levels tended to be lower in Met-depleted embryos than in controls (Fig. S2C). Mad, Medea and Smox expression in Met-depleted embryos was not significantly different from that measured in controls (Fig. S2D). Finally, expression of hb, Kr and otd was also similar in Met-depleted embryos and in controls (Fig. S2E).

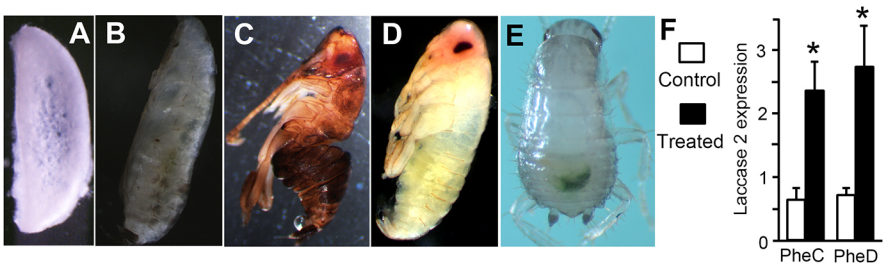

Fig. 2. Embryo phenotypes resulting from maternal RNAi of Kr-h1 in *B. germanica*. (A) Phenotype A. (B) Phenotype B. (C) Phenotype C. (D) Phenotype D. (E) Normal freshly eclosed first instar nymph. (F) Expression of laccase 2 in phenotype C (PheC) and phenotype D (PheD) embryos; PheC and PheD embryos were obtained from Kr-h1-depleted oothecae on day 19, and compared with freshly emerged first instar nymphs from oothecae formed by control females (measurements were carried out 19 days after ootheca formation in both cases). Each measurement represents three biological replicates and results of qRT-PCR are expressed as copies of the examined transcript per 1000 copies of *BgActin-5c* mRNA. Data are presented as mean±s.e.m. *$P<0.05$ compared to controls, calculated on the basis of the REST (Pfaffl et al., 2002).

Development (2017) 144, 4637-4644 doi:10.1242/dev.152827

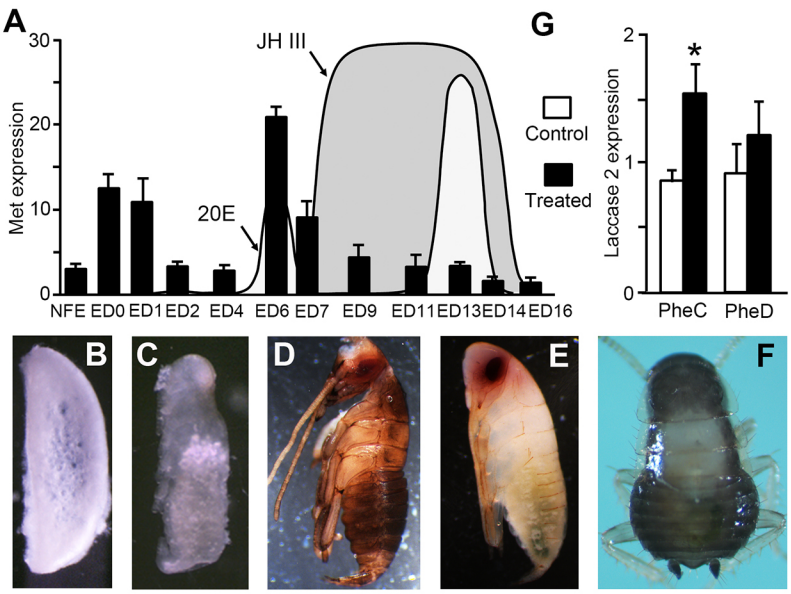

Fig. 3. Expression of Met in embryos of *B. germanica* and effects of maternal RNAi. (A) *Met* mRNA levels in NFEs, and in embryos of different ages from ED0 to ED16; superimposed are the patterns of 20E and JH III, according to the data of Maestro et al. (2005) and Maestro et al. (2010), respectively. (B) Phenotype A. (C) Phenotype B. (D) Phenotype C. (E) Phenotype D. (F) Normal freshly eclosed first instar nymph. (G) Expression of laccase 2 in phenotype C (PheC) and phenotype D (PheD) embryos; PheC and PheD embryos were obtained from Met-depleted oothecae on day 19, and compared with freshly emerged first instar nymphs from oothecae formed by control females (measurements were carried out 19 days after ootheca formation in both cases). Each measurement represents three biological replicates and results of qRT-PCR are expressed as copies of the examined transcript per 1000 copies of *BgActin-5c* mRNA. Data are presented as mean± s.e.m. **P*<0.05 compared to controls, calculated on the basis of the REST (Pfaffl et al., 2002).

Females treated with dsMock (*n*=32) formed the first ootheca on day 8 of adult life, which contained viable embryos that hatched 18 days later, giving normal first instar nymphs. In the parallel group of dsMet-treated specimens (*n*=45), oothecae were also formed on day 8 of adult life. Forty of these oothecae (88.9%) hatched on day 18, giving apparently well-formed first instar nymphs, whereas five of them (11.1%) were transported beyond day 18 without hatching (Table S1). On day 19, we dissected the five oothecae that did not hatch and then examined 190 of their embryos. A total of 47 of them (24.7%) matched phenotype A (Fig. 3B), 65 (34.2%) were phenotype B (Fig. 3C), 53 (27.9%) were phenotype C (Fig. 3D) and 25 (13.2%) were phenotype D (Fig. 3E). Again, when the oothecae were opened and the chorion broken, most of the phenotype D specimens behaved normally in terms of motility and showed the same morphology as freshly emerged first instar nymphs (Fig. 3F) (see also Table S2). None of the oothecae formed by dsMet-treated females were dropped between days 2 and 3. Nevertheless, we found phenotype A specimens in oothecae that did not hatch on day 18. Embryos with phenotype B were similar to those observed in the dsKr-h1 experiments (Fig. 2B), and could be the result of the concomitant reduction of Kr-h1 and BR-C expression (Fig. S2B). Laccase 2 expression was significantly higher in phenotype C embryos than in controls, and tended to be higher in phenotype D embryos than in controls (Fig. 3G).

Disrupting JH biosynthesis: JHAMT depletion

The pattern for *JHAMT* transcript levels in the embryo is shown in Fig. 4A. There is significant expression from NFE stage to ED2, including the highest levels measured on ED1, when there is no detectable JH (Maestro et al., 2010). The expression during the cycle of JH production, from ED6 to ED16, is somewhat fluctuating. Maternal RNAi resulted in depleted levels of *JHAMT*, as measured at ED6 (Fig. S3A). On ED9, *JHAMT* transcript levels were still significantly lower in treated embryos than in controls, but on ED13, they were similar in both groups (Fig. S3A).

On ED6, transcript levels of *Met*, *Kr-h1* and *BR-C* were reduced in JHMT-depleted embryos (Fig. S3B), as expected. At this age, PCNA and Zelda expression levels in these embryos were comparable to those measured in the controls (Fig. S3C), similar to what was observed for Mad, Medea and Smox expression (Fig. S3D). Finally, expression of hb, Kr and otd was also similar in JHAMT-depleted embryos and in controls (Fig. S3E).

All control (dsMock-treated) females (*n*=50) formed an ootheca on day 8 of adult life, containing normal embryos, which resulted in nymphs that eclosed 18 days later. Females treated in parallel with dsJHAMT (*n*=68) also formed apparently normal oothecae on day 8. Forty-eight of them (70.6%) gave apparently normal first instar nymphs that eclosed on day 18. Eight of the oothecae (11.8%) were spontaneously dropped between days 2 and 3 of ootheca transport (12-17% embryogenesis), whereas 12 of them (17.6%) were transported beyond day 18 without hatching (Table S1).

We studied 148 embryos from the eight oothecae that had dropped between days 2 and 3. They were between Tanaka stages 1 and 2 and showed a number of energids accumulating in the ventral area and the germ-band anlage, similar to those of controls on ED2 (Fig. 4B,C), which cellularized upon reaching the egg membrane. In dsJHAMT-depleted embryos, Smox and Otd expression was significantly higher than in controls, and expression of PCNA, Mad and Medea tended to be higher than in controls, whereas expression of Zelda, hb and Kr was practically unaffected (Fig. 4D-F).

On day 19, we dissected eight of the 12 oothecae that were transported beyond day 18 without hatching and then examined 195 of their embryos. A total of 114 of them (58.5%) presented phenotype A (Fig. 5A), 44 (22.6%) were phenotype B (Fig. 5B), 3 (1.5%) were phenotype C (Fig. 5C) and 34 (17.4%) were phenotype D (Fig. 5D). The latter group exhibited the morphology and behavior of a normal, freshly emerged, first instar nymph (Fig. 5E) when artificially released from the chorion (see also Table S2). Phenotype A embryos corresponded to those from oothecae dropped between days 2 and 3. Embryos with phenotype B were similar to those observed after dsKr-h1 and dsMet treatments, and could be the result of the low levels of BR-C triggered by them (Fig. S1B). The small number of specimens with phenotype C prevented mRNA measurements of laccase 2, but in phenotype D, transcript levels of this gene tended to be higher in JHAMT-depleted embryos than in controls (Fig. 5F).

DISCUSSION

Patterns of expression and epistatic relationships

The significant amounts of *Kr-h1*, *Met* and *JHAMT* transcripts present in NFE, ED0 and ED1 of *B. germanica* indicate that they derive from a

Development (2017) 144, 4637-4644 doi:10.1242/dev.152827

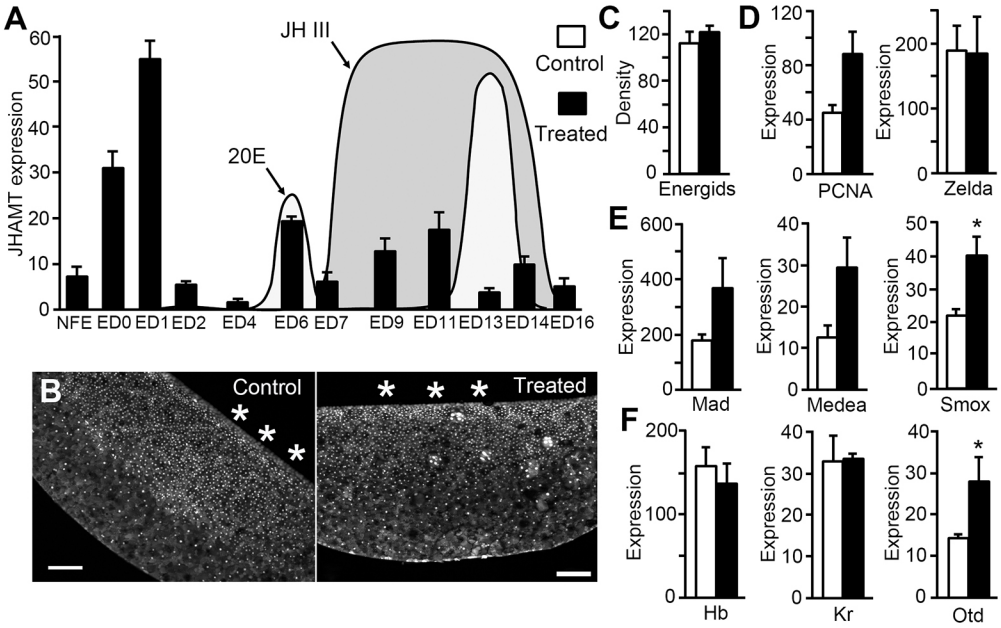

Fig. 4. Expression of JHAMT in embryos of *Blattella germanica*, and effects of maternal RNAi on ED2. (A) *JHAMT* mRNA levels in NFEs, and in embryos of different ages from ED0 to ED16; superimposed are the patterns of 20E and JH III, according to the data of Maestro et al. (2005) and Maestro et al. (2010), respectively. (B) Control and treated (JHAMT-depleted) embryos showing the accumulation of energids in the ventral side (asterisks). Scale bars: 200 µm. (C) Density of energids (number of energids in 0.10 mm^2) in control and treated (JHAMT-depleted) embryos. (D) Expression of PCNA and Zelda. (E) Expression of the Smads of the TGF-β pathways, Mad, Medea and Smox. (F) Expression of the gap genes *hb*, *Kr* and *otd*. Each measurement represents three biological replicates and results of qRT-PCR are expressed as copies of the examined transcript per 1000 copies of *BgActin-5c* mRNA. Data are presented as mean±s.e.m. **P*<0.05 compared to controls, calculated on the basis of the REST (Pfaffl et al., 2002).

maternal origin. The occurrence of these transcripts so early in embryo development is intriguing, as JH starts being detected later, around the dorsal closure stage (Maestro et al., 2010). JH quantification was carried out with gas chromatography-mass spectrometry, with an absolute detection limit of 0.02 pmol, and measurements on ED0, ED2 and ED4 using pools of eight embryos did not detect any JH amount. This means that if there is JH at these ages, the titer should be <0.003 pmol per embryo. We cannot discard that JH could be present at these low amounts, especially taking into account that the embryo represents a very low percentage of the egg mass at these very early stages. We can also consider that methyl farnesoate (MF), which can bind to the JH receptor with low affinity (Jindra et al., 2015a,b), but was not measured by Maestro et al. (2010), might be a possible effector of JH signaling in early embryos. MF has been detected in embryos of different cockroaches including *B. germanica* (Li, 2007) after the dorsal closure stage (~45% development in most species), and titers are ≥10 times lower than those of JH. In *Diploptera punctata*, in which the dorsal closure exceptionally occurs at 20% development, JH and MF can be detected only from 40% development, when the CA are well formed and functional (Stay et al., 2002), but the titers of MF are ~30 times lower than those of JH.

Our patterns of expression show that *Kr-h1*, *Met* and *JHAMT* transcripts are then detected again between ED6 and ED16, when a cycle of JH produced by the CA is clearly measurable (Maestro et al., 2010). In *B. mori* embryos, there are significant amounts of *Kr-h1*, the two *Met* paralogs of this species and *JHAMT* transcripts in very early stages of embryo development, which would correspond to maternal loading. Subsequently, these transcripts are detected again between 96 and 240 h after oviposition, coinciding with a period of detectable JH (Daimon et al., 2015).

Our transcript measurements on ED6 indicated that RNAi treatments reduced the respective mRNA levels of *Kr-h1*, *Met* and

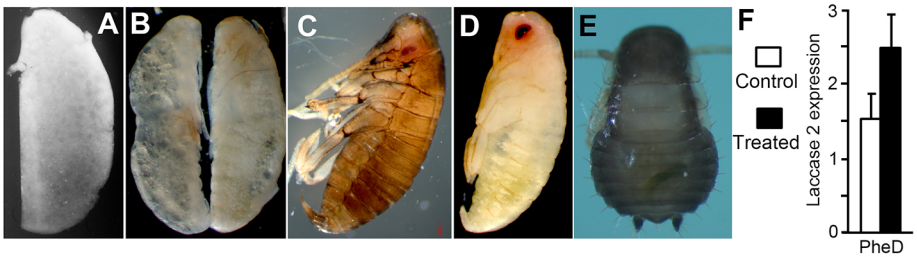

Fig. 5. Embryo phenotypes resulting from maternal RNAi of JHAMT in *B. germanica*. (A) Phenotype A. (B) Phenotype B. (C) Phenotype C. (D) Phenotype D. (E) Normal freshly eclosed first instar nymph. (F) Expression of laccase 2 in phenotype D (PheD) embryos; PheD embryos were obtained from JHAMT-depleted oothecae on day 19, and compared with freshly emerged first instar nymphs from oothecae formed by control females (measurements were carried out 19 days after ootheca formation in both cases). Each measurement represents three biological replicates and results of qRT-PCR are expressed as copies of the examined transcript per 1000 copies of *BgActin-5c* mRNA. Data are presented as mean±s.e.m.

Development (2017) 144, 4637-4644 doi:10.1242/dev.152827

JHAMT (~60%, 70% and 85%, respectively). Given the phenotypes obtained, we presume that double-stranded RNA (dsRNA) treatment in 5-day-old adult females reduced the maternal transcripts in treated females (those measured at NFE stage, ED0 and ED1) and later the zygotic transcripts in the embryo (after ED2, when the maternal to zygotic transition occurs). The measurements of targeted transcripts in ED6 showed that the epistatic relationships between these genes were as expected according to the axis JHAMT (JH)-Met-Kr-h1 that operates in postembryonic development (Belles and Santos, 2014; Jindra et al., 2015a,b). The same epistatic relationships have been also reported during *B. mori* embryogenesis (Daimon et al., 2015), implying that the basic JH signaling pathway is conserved in hemimetabolan and holometabolan embryos. In *B. germanica* nymphs, BR-C expression is stimulated by JH (Huang et al., 2013). In embryos, BR-C is consistently expressed during the period of JH production (Piulachs et al., 2010), and our results indicate that its expression is also JH stimulated, downstream of Kr-h1. In holometabolan species, BR-C is generally repressed by JH, at least during young larval instars (Zhou and Riddiford, 2002). However, the elimination of JH signaling in young larvae of *B. mori* does not trigger an increase in BR-C expression (Daimon et al., 2015). Therefore the authors suggested that a 'competence factor' is additionally needed to trigger BR-C expression before pupal formation. In *B. mori* embryos, the pattern of *BR-C* mRNA shows relatively high levels in very early stages, which are possibly of maternal origin, and rather low levels during the cycle of JH production (Daimon et al., 2015). However, *BR-C* mRNA levels in the embryo are not modified in mutants for JH synthesis and signaling genes (Daimon et al., 2015), which implies that JH does not affect BR-C expression during *B. mori* embryogenesis.

Formation of the germ-band anlage

A number of females treated with dsRNA targeting *Kr-h1* or *JHMT* dropped the ootheca ~2 days after its formation (Table S1), between stages 1 and 2 of Tanaka (1976). Moreover, between ~40% and 60% of Kr-h1- or JHAMT-depleted embryos contained in oothecae that did not hatch on day 18 (Table S2), interrupted development around day 2, while forming the germ-band anlage. Our data suggest that Kr-h1 and JHAMT play different roles in embryos between stage 1 and 2. Kr-h1 appears to promote PCNA expression, which is required for cell cycle progression and cell proliferation and has been associated with nuclear division cycles in early *D. melanogaster* embryogenesis (Yamaguchi et al., 1991). The relatively low number of energids observed in Kr-h1-depleted embryos would then be a consequence of the low PCNA expression. Importantly, Kr-h1 would also promote the expression of Zelda in early *B. germanica* embryogenesis. Zelda might be a crucial gene in the maternal to zygotic transition, as shown in *D. melanogaster* (Liang et al., 2008; Schulz et al., 2015; Sun et al., 2015). If Zelda has the same function in *B. germanica* as in *D. melanogaster*, then divergences in the expression of gap genes in Kr-h1-depleted embryos might be caused by low Zelda expression, which would have led to deregulation of the early zygotic gene expression and epistasis. On the other hand, JHAMT appears to exert a negative regulation on the expression of Smads in TGF-β pathways, which are important for embryonic development (Deignan et al., 2016), and on the gap gene *otd*, the function of which is crucial in early embryogenesis in short and long germ-band insect embryos (Lynch et al., 2012).

Although none of the oothecae formed by dsMet-treated females were dropped between days 2 and 3, we presume that Met has functions in early embryo; first, because Met is consistently expressed in ED0 and ED1; and second, because we found phenotype A embryos (thus with development interrupted between Tanaka stages 1 and 2) in unhatched oothecae formed by dsMet-treated females.

Mid-embryo development

In Kr-h1-depleted specimens, a number of oothecae were dropped between days 7 and 15 (Table S1). Then, a significant percentage of the oothecae formed by Kr-h1-, Met- and JHAMT-depleted females were transported beyond day 18 without hatching (Table S1). In these unhatched oothecae, we found that between 23% and 34% of the embryos interrupted development between Tanaka stages 10 to 16 (Table S2), producing what we called phenotype B (Table S2). These embryos exhibited various malformations, the most common being an unsealed dorsal closure, a reduction in the size of the abdomen, shorter appendages and imperfect eyes. Most of the phenotype B embryos were reminiscent of those observed in BR-C-depleted embryos previously reported (Piulachs et al., 2010). Because Kr-h1, Met and JHAMT depletion in embryos reduced the expression of BR-C, our interpretation is that the diverse phenotypes observed in mid-embryo stages are caused, at least in part, by the low levels of BR-C.

Late embryo development

A significant number of oothecae from females treated with dsKr-h1, Met or JHAMT were transported beyond day 18 without hatching (Table S1). Between 2% and 28% of the embryos in these oothecae had experienced premature tanning (phenotype C), and between 13% and 21% were apparently normal nymphs, but they did not hatch (phenotype D) (Table S2).

Previous work with the cricket *A. domesticus* showed that premature exposure of embryos to JH resulted in a precocious differentiation of nymphal features (Erezyilmaz et al., 2004). These observations might suggest that reducing JH signaling in *B. germanica* in mid to late embryos would impair the formation of nymphal features during the deposition of the third embryonic cuticle (the first nymphal cuticle, indeed), which occurs after the third ecdysone peak of ED13 (Maestro et al., 2005), when JH levels are high (Maestro et al., 2010). However, embryos from RNAi-treated females that reached the deposition of the third embryonic cuticle showed the current nymphal features, such as sclerotized mandibles and correctly patterned nymphal microsculpture and chaetotaxy. These results, however, must be interpreted with caution as the *Kr-h1*, *Met* and *JHAMT* transcripts recovered normal levels between ED9 and ED13 after the RNAi. Therefore, we cannot discard the hypothesis that JH contributes to the formation of the nymph at the deposition of the third embryonic cuticle, given that we cannot discard that Kr-h1, Met or JHAMT protein levels around ED13 in the respective experiments, even if reduced, were high enough to eventually allow a normal nymphal morphogenesis.

In phenotypes C and D, we measured abnormally high levels of laccase 2, which is a key factor in cuticle tanning in postembryonic molts (Arakane et al., 2005; Elias-Neto et al., 2010; Sugumaran and Barek, 2016). Moreover, laccase 2 is required for eggshell tanning in the mosquito *Aedes albopictus* (Wu et al., 2013). In ED13 *B. germanica*, the third ecdysone peak that elicits the nymphal cuticle deposition is produced in a context of high JH titers (Maestro et al., 2010). Phenotypes C and D suggest that JH signaling inhibits laccase 2 expression in this context, thus precluding a premature cuticle tanning. The inhibitory action of JH on laccase 2 is not unprecedented: Cao et al. (2014) reported that the JH analog methoprene represses laccase 2 expression in larvae of the cotton

Development (2017) 144, 4637-4644 doi:10.1242/dev.152827

bollworm, *Helicoverpa armigera*. Obvious premature sclerotization of phenotype C animals immediately suggests that they will not be able to hatch. The problems of hatching of phenotype D animals could also be explained, at least in part, by the abnormally high expression levels of laccase 2.

JH signaling in hemimetabolan and holometabolan embryos

Our observations of impaired hatchability of embryos are reminiscent of those of Aboulafia-Baginsky et al. (1984), who showed that 39% of eggs from *L. migratoria* treated with precocene in late stages of embryogenesis did not hatch. Therefore, involvement of JH signaling in hatching appears to be conserved in hemimetabolan insects, at least in orthopterans and dictyopterans. The work of Daimon et al. (2015) in *B. mori* evidenced that only 20% of the embryos hatched normally after knocking out JHAMT and Met. However, the unhatched embryos were able to emerge as apparently normal first instar larvae if they were artificially dechorionated (Daimon et al., 2015). These results are similar to our observations regarding the impaired hatchability of Kr-h1-, Met- and JHAMT-depleted embryos from *B. germanica*, and suggest that the roles of JH signaling in embryo hatchability are conserved in hemimetabolan and holometabolan insects. It remains to be ascertained whether more or less strong premature tanning might also be the cause, at least partial, of the diminished hatchability in JH-depleted embryos of *L. migratoria* and *B. mori*.

In *B. mori*, homozygous mutant embryos for Met and JHAMT were obtained from sibling crosses of heterozygous adult moths (Daimon et al., 2015). As heterozygous females produce both wild-type and mutated transcripts of *Met* and *JHAMT*, then both must be maternally deposited in embryos and work during the earliest embryonic stages. Therefore, these experiments would not show whether maternal *Met* and *JHAMT* transcripts play a role in prezygotic stages of embryonic development in *B. mori*. With regards to the JH signaling that occurs from mid to late embryogenesis in *B. mori* (Daimon et al., 2015) and *B. germanica* (present results), the available data imply that it does not have a morphogenetic role in *B. mori*, whereas phenotypes with morphological malformations (although at a low penetrance) were observed between stages 10 and 15 in embryos of *B. germanica* with depleted transcripts of *Kr-h1*, *Met* and *JHAMT*. Given that these phenotypes are similar to those found in BR-C-depleted embryos (Piulachs et al., 2010), we presume that they derive, at least in part, from the lower levels of BR-C expression derived from Kr-h1, Met or JHAMT depletion. Moreover, we observed that BR-C expression is stimulated by JH in *B. germanica* embryos, as occurs in nymphs (Huang et al., 2013), whereas, in contrast, JH does not appear to affect the (low) expression of BR-C in *B. mori* embryos (Daimon et al., 2015). Taken together, the observations suggest that the stimulatory role of JH signaling on BR-C expression and the morphogenetic functions of JH in hemimetabolan embryos (possibly mediated by BR-C, at least in part), were lost in holometabolan embryos. If so, then this might have been an important driver for the evolution towards holometabolan metamorphosis.

MATERIALS AND METHODS

Insects and dissections

B. germanica specimens were from a colony reared in the dark at 30±1°C and 60-70% relative humidity. Newly emerged females were maintained with males during the first gonadotrophic cycle, and mating was confirmed at the end of experiments by assessing the presence of spermatozoids in the spermathecae. For dissections and tissue sampling, specimens were anesthetized with carbon dioxide. For RNA extractions, we used NFEs (see below), entire oothecae (to establish the expression patterns along embryogenesis and in oothecae from treated females dropped between days 2 and 3), or individual embryos dissected out from artificially opened oothecae.

RNA extraction and retrotranscription to cDNA

RNA extractions were performed with a Gen Elute Mammalian Total RNA kit (Sigma-Aldrich). An amount of 100 ng from each RNA extraction was treated with DNase (Promega) and reverse transcribed with Superscript II reverse transcriptase (Invitrogen) and random hexamers (Promega). RNA quantity and quality were estimated by spectrophotometric absorption using a NanoDrop Spectrophotometer ND-1000 (NanoDrop Technologies).

Quantitative real-time PCR

Quantitative real-time PCR (qRT-PCR) measurements were performed in triplicate in an iQ5 Real-Time PCR Detection System (Bio-Rad Laboratories), using SYBR Green Supermix (iTaq Universal Supermix; Applied Biosystems). A control without a template was included in all batches. The primers used to measure the transcripts studied are indicated in Table S3. The efficiency of the primer sets was first validated by constructing a standard curve through four serial dilutions. mRNA levels were calculated relative to *BgActin-5c* expression, using the Bio-Rad iQ5 Standard Edition Optical System Software (version 2.0). Results are given as copies of mRNA per 1000 copies of *BgActin-5c* mRNA.

RNA interference

Detailed procedures for dsRNA preparation were as described previously (Ciudad et al., 2006). The dsRNAs used to target *Kr-h1*, *Met* and *JHAMT* were those described in previous papers by Lozano and Belles (2011), Lozano and Belles (2014) and Dominguez and Maestro (2017), respectively. A dsRNA from *Autographa californica* nucleopoydrovirus was used for control treatments (dsMock). The primers used to prepare the dsRNAs are detailed in Table S3. Maternal RNAi treatments were carried out essentially as previously reported (Piulachs et al., 2010). A volume of 1 µl of dsRNA solution (3 µg/µl) was injected into the abdomen of 5-day-old adult females. Then, the effects of the treatment were examined in the first oothecae formed by treated and control females 6, 9 and 13 days after oviposition.

Examination of embryos

Expression studies were carried out in NFEs, and in embryos on day 0, 1, 2, 4, 6, 7, 9, 11, 13, 14 and 16 (ED0 to ED16). NFEs are eggs obtained just before descending the oviduct to which the remains of follicular epithelium were removed. They should contain only maternal transcripts. ED0 to ED2 cover the maternal to zygotic transition; ED3, ED6 and ED13 coincide with respective pulses of 20-hydroxyecdysone (20E) (Maestro et al., 2005); and ED6 to ED16 cover the period of JH production (Maestro et al., 2010). To examine the embryos microscopically, the oothecae were opened after 5 min in a water bath at 95°C and the embryos were dechorionated and individualized. Then, they were fixed in 4% paraformaldehyde, permeabilized in PBS+0.2% Tween (PBT) and incubated for 10 min in 1 µg/ml DAPI in PBT. They were then mounted in Mowiol 4-88 (Calbiochem) and examined and photographed using epifluorescence with an AxioImager Z1 microscope (ApoTome System, Zeiss). Embryo stages were established using the criteria and nomenclature of Tanaka (1976). To estimate the energid density in stage 2 embryos, we counted the number of energids included in a 0.10 mm^2 rectangle placed in the middle of the egg in lateral view, equidistant from the poles and from the ventral and dorsal sides.

Acknowledgements

We thank Takaaki Daimon for useful comments and suggestions to a first version of the manuscript. We are grateful to Guillem Ylla for assistance with transcriptome comparisons and searching for genes in the *B. germanica* genome, which is available at https://www.hgsc.bcm.edu/arthropods/german-cockroach-genome-project, as provided by the Baylor College of Medicine Human Genome Sequencing Center.

Competing interests

The authors declare no competing or financial interests.

Author contributions

Conceptualization: A.F.-N., X.B.; Methodology: A.F.-N., X.B.; Formal analysis: A.F.-N., X.B.; Investigation: A.F.-N., X.B.; Resources: X.B.; Writing - original draft: X.B.; Writing - review & editing: X.B.; Supervision: X.B.; Project administration: X.B.; Funding acquisition: X.B.

Funding

The work was supported by the Ministerio de Economía y Competitividad [CGL2012-36251 and CGL2015-64727-P to X.B., and a predoctoral fellowship to A.F.-N.] and Generalitat de Catalunya [2014 SGR 619].

Supplementary information

Supplementary information available online at
http://dev.biologists.org/lookup/doi/10.1242/dev.152827.supplemental

References

Aboulafia-Baginsky, N., Pener, M. P. and Staal, G. B. (1984). Chemical allatectomy of late *Locusta* embryos by a synthetic precocene and its effect on hopper morphogenesis. *J. Insect Physiol.* **30**, 839-852.

Arakane, Y., Muthukrishnan, S., Beeman, R. W., Kanost, M. R. and Kramer, K. J. (2005). Laccase 2 is the phenoloxidase gene required for beetle cuticle tanning. *Proc. Natl. Acad. Sci. USA* **102**, 11337-11342.

Belles, X. (2011). *Origin and Evolution of Insect Metamorphosis*. *eLS*. Chichester: John Wiley & Sons.

Belles, X. and Santos, C. G. (2014). The MEKRE93 (Methoprene tolerant-Krüppel homolog 1-E93) pathway in the regulation of insect metamorphosis, and the homology of the pupal stage. *Insect Biochem. Mol. Biol.* **52**, 60-68.

Cao, Z., Liu, X., An, S. and Jiang, J. (2014). Molecular identification of laccase 2 gene in the cotton bollworm, *Helicoverpa armigera* (Lepidoptera: Noctuidae). *Acta Entomol. Sin.* **57**, 150-160.

Ciudad, L., Piulachs, M.-D. and Belles, X. (2006). Systemic RNAi of the cockroach vitellogenin receptor results in a phenotype similar to that of the *Drosophila* yolkless mutant. *FEBS J.* **273**, 325-335.

Daimon, T., Uchibori, M., Nakao, H., Sezutsu, H. and Shinoda, T. (2015). Knockout silkworms reveal a dispensable role for juvenile hormones in holometabolous life cycle. *Proc. Natl. Acad. Sci. USA* **112**, E4226-E4235.

Deignan, L., Pinheiro, M. T., Sutcliffe, C., Saunders, A., Wilcockson, S. G., Zeef, L. A. H., Donaldson, I. J. and Ashe, H. L. (2016). Regulation of the BMP signaling-responsive transcriptional network in the *Drosophila* embryo. *PLoS Genet.* **12**, e1006164.

Dominguez, C. V. and Maestro, J. L. (2017). Expression of juvenile hormone acid *O*-methyltransferase and juvenile hormone synthesis in *Blattella germanica*. *Insect Sci.*, doi: 10.1111/1744-7917.12467.

Elias-Neto, M., Soares, M. P. M., Simões, Z. L. P., Hartfelder, K. and Bitondi, M. M. G. (2010). Developmental characterization, function and regulation of a Laccase2 encoding gene in the honey bee, *Apis mellifera* (Hymenoptera, Apinae). *Insect Biochem. Mol. Biol.* **40**, 241-251.

Enslee, E. C. and Riddiford, L. M. (1977). Morphological effects of juvenile hormone mimics on embryonic development in the bug, *Pyrrhocoris apterus*. *Wilhelm Roux's Arch. Dev. Biol.* **181**, 163-181.

Erezyilmaz, D. F., Riddiford, L. M. and Truman, J. W. (2004). Juvenile hormone acts at embryonic molts and induces the nymphal cuticle in the direct-developing cricket. *Dev. Genes Evol.* **214**, 313-323.

Huang, J.-H., Lozano, J. and Belles, X. (2013). Broad-complex functions in postembryonic development of the cockroach *Blattella germanica* shed new light on the evolution of insect metamorphosis. *Biochim. Biophys. Acta* **1830**, 2178-2187.

Jindra, M., Belles, X. and Shinoda, T. (2015a). Molecular basis of juvenile hormone signaling. *Curr. Opin. Insect Sci.* **11**, 39-46.

Jindra, M., Uhlirova, M., Charles, J. P., Smykal, V. and Hill, R. J. (2015b). Genetic evidence for function of the bHLH-PAS protein Gce/Met as a juvenile hormone Receptor. *PLoS Genet.* **11**, e1005394.

Kelman, Z. (1997). PCNA: structure, functions and interactions. *Oncogene* **14**, 629-640.

Konopová, B. and Zrzavý, J. (2005). Ultrastructure, development, and homology of insect embryonic cuticles. *J. Morphol.* **264**, 339-362.

Li, X. (2007). Juvenile hormone and methyl farnesoate production in cockroach embryos in relation to dorsal closure and the reproductive modes of different species of cockroaches. *Arch. Insect Biochem. Physiol.* **66**, 159-168.

Liang, H.-L., Nien, C.-Y., Liu, H.-Y., Metzstein, M. M., Kirov, N. and Rushlow, C. (2008). The zinc-finger protein Zelda is a key activator of the early zygotic genome in *Drosophila*. *Nature* **456**, 400-403.

Lozano, J. and Belles, X. (2011). Conserved repressive function of Krüppel homolog 1 on insect metamorphosis in hemimetabolous and holometabolous species. *Sci. Rep.* **1**, 163.

Lozano, J. and Belles, X. (2014). Role of methoprene-tolerant (Met) in adult morphogenesis and in adult ecdysis of *Blattella germanica*. *PLoS ONE* **9**, e103614.

Lynch, J. A., El-Sherif, E. and Brown, S. J. (2012). Comparisons of the embryonic development of *Drosophila*, *Nasonia*, and *Tribolium*. *Wiley Interdiscip. Rev. Dev. Biol.* **1**, 16-39.

Maestro, O., Cruz, J., Pascual, N., Martín, D. and Bellés, X. (2005). Differential expression of two RXR/ultraspiracle isoforms during the life cycle of the hemimetabolous insect *Blattella germanica* (Dictyoptera, Blattellidae). *Mol. Cell. Endocrinol.* **238**, 27-37.

Maestro, J. L., Pascual, N., Treiblmayr, K., Lozano, J. and Bellés, X. (2010). Juvenile hormone and allatostatins in the German cockroach embryo. *Insect Biochem. Mol. Biol.* **40**, 660-665.

Matolín, S. and Gelbic, I. (1975). The ovicidal and sterilant effects of juvenoids on the codling moth, *Cydia pomonella* (Lepidoptera, Tortricidae). *Acta Entomol. Bohemoslov.* **72**, 360-369.

Pfaffl, M. W., Horgan, G. W. and Dempfle, L. (2002). Relative expression software tool (REST) for group-wise comparison and statistical analysis of relative expression results in real-time PCR. *Nucleic Acids Res.* **30**, e36.

Piulachs, M.-D., Pagone, V. and Bellés, X. (2010). Key roles of the Broad-Complex gene in insect embryogenesis. *Insect Biochem. Mol. Biol.* **40**, 468-475.

Pratt, G. E., Jennings, R. C., Hamnett, A. F. and Brooks, G. T. (1980). Lethal metabolism of precocene-I to a reactive epoxide by locust corpora allata. *Nature* **284**, 320-323.

Rohdendorf, E. B. and Sehnal, F. (1973). Inhibition of reproduction and embryogenesis in the firebrat, *Thermobia domestica*, by juvenile hormone analogues. *J. Insect Physiol.* **19**, 37-56.

Santos, C. G., Fernandez-Nicolas, A. and Belles, X. (2016). Smads and insect hemimetabolan metamorphosis. *Dev. Biol.* **417**, 104-113.

Schulz, K. N., Bondra, E. R., Moshe, A., Villalta, J. E., Lieb, J. D., Kaplan, T., McKay, D. J. and Harrison, M. M. (2015). Zelda is differentially required for chromatin accessibility, transcription factor binding, and gene expression in the early *Drosophila* embryo. *Genome Res.* **25**, 1715-1726.

Smith, R. F. and Arking, R. (1975). The effects of juvenile hormone analogues on the embryogenesis of *Drosophila melanogaster*. *J. Insect Physiol.* **21**, 723-732.

Stay, B., Zhang, J. R. and Tobe, S. S. (2002). Methyl farnesoate and juvenile hormone production in embryos of *Diploptera punctata* in relation to innervation of corpora allata and their sensitivity to allatostatin. *Peptides* **23**, 1981-1990.

Sugumaran, M. and Barek, H. (2016). Critical analysis of the melanogenic pathway in insects and higher animals. *Int. J. Mol. Sci.* **17**, 1753.

Sun, Y., Nien, C.-Y., Chen, K., Liu, H.-Y., Johnston, J., Zeitlinger, J. and Rushlow, C. (2015). Zelda overcomes the high intrinsic nucleosome barrier at enhancers during *Drosophila* zygotic genome activation. *Genome Res.* **25**, 1703-1714.

Tanaka, A. (1976). Stages in the embryonic development of the German cockroach, *Blattella germanica* Linné (Blattaria, Blattellidae). *Kontyû, Tokyo* **44**, 1703-1714.

Truman, J. W. and Riddiford, L. M. (1999). The origins of insect metamorphosis. *Nature* **401**, 447-452.

Truman, J. W. and Riddiford, L. M. (2002). Endocrine insights into the evolution of metamorphosis in insects. *Annu. Rev. Entomol.* **47**, 467-500.

Wu, X., Zhan, X., Gan, M., Zhang, D., Zhang, M., Zheng, X., Wu, Y., Li, Z. and He, A. (2013). Laccase 2 is required for sclerotization and pigmentation of *Aedes albopictus* eggshell. *Parasitol. Res.* **112**, 1929-1934.

Yamaguchi, M., Date, T. and Matsukage, A. (1991). Distribution of PCNA in *Drosophila* embryo during nuclear division cycles. *J. Cell Sci.* **100**, 729-733.

Zhou, X. and Riddiford, L. M. (2002). Broad specifies pupal development and mediates the "status quo" action of juvenile hormone on the pupal-adult transformation in *Drosophila* and *Manduca*. *Development* **129**, 2259-2269.

Juvenile hormone signaling in short germ-band hemimetabolan embryos

Ana Fernandez-Nicolas and Xavier Belles

SUPPLEMENTARY INFORMATION

Fig. S1. Effects of maternal RNAi of Kr-h1 in embryos of *Blattella germanica*.

Fig. S2. Effects of maternal RNAi of Met in embryos of *Blattella germanica*.

Fig. S3. Effects of maternal RNAi of JHAMT in embryos of *Blattella germanica*.

Table S1. Summary of the effects of maternal RNAi of JHMT, Met or Kr-h1 on ootheca fate.

Table S2. Summary of the phenotypes observed in not hatched oothecae from females treated with dsRNA targeting JHMT, Met or Kr-h1, examined on day 19.

Table S3. Primers used for transcript measurements and to prepare dsRNAs.

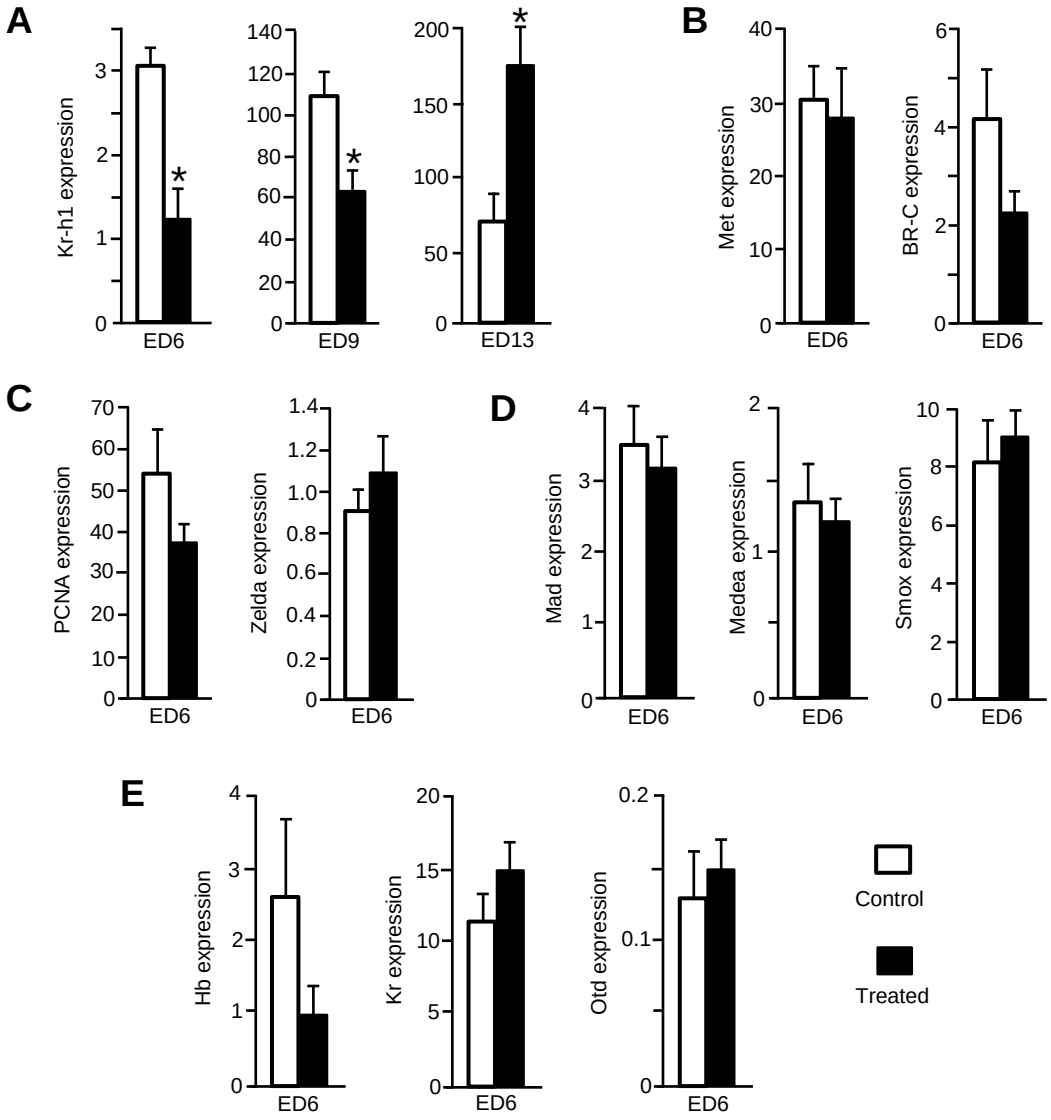

Fig. S1. Effects of maternal RNAi of Kr-h1 in embryos of *Blattella germanica*. (A) Kr-h1 mRNA levels; dsKr-h1 (or dsMock, in controls) was administered on 5-day-old adult females, and measurements were carried out on ED6, ED9 and ED13. (B) Effects on the expression of Met and BR-C, measured on ED6, when Kr-h1 transcripts are more effectively depleted. (C) Expression of PCNA and Zelda on ED6. (D) Expression of the Smads of the TGF-β pathways, Mad, Medea and Smox on ED6. (E) Expression of gap genes Hunchback (Hb), Krüppel (Kr) and Orthodenticle (Otd) on ED6. Each measurement represents three biological replicates and results of qRT-PCR are expressed as copies of the examined transcript per 1000 copies of BgActin-5c mRNA. Data are represented as the mean ± SEM. The asterisk indicates statistically significant differences with respect to controls ($p < 0.05$), calculated on the basis of the REST (Pfaffl et al., 2002).

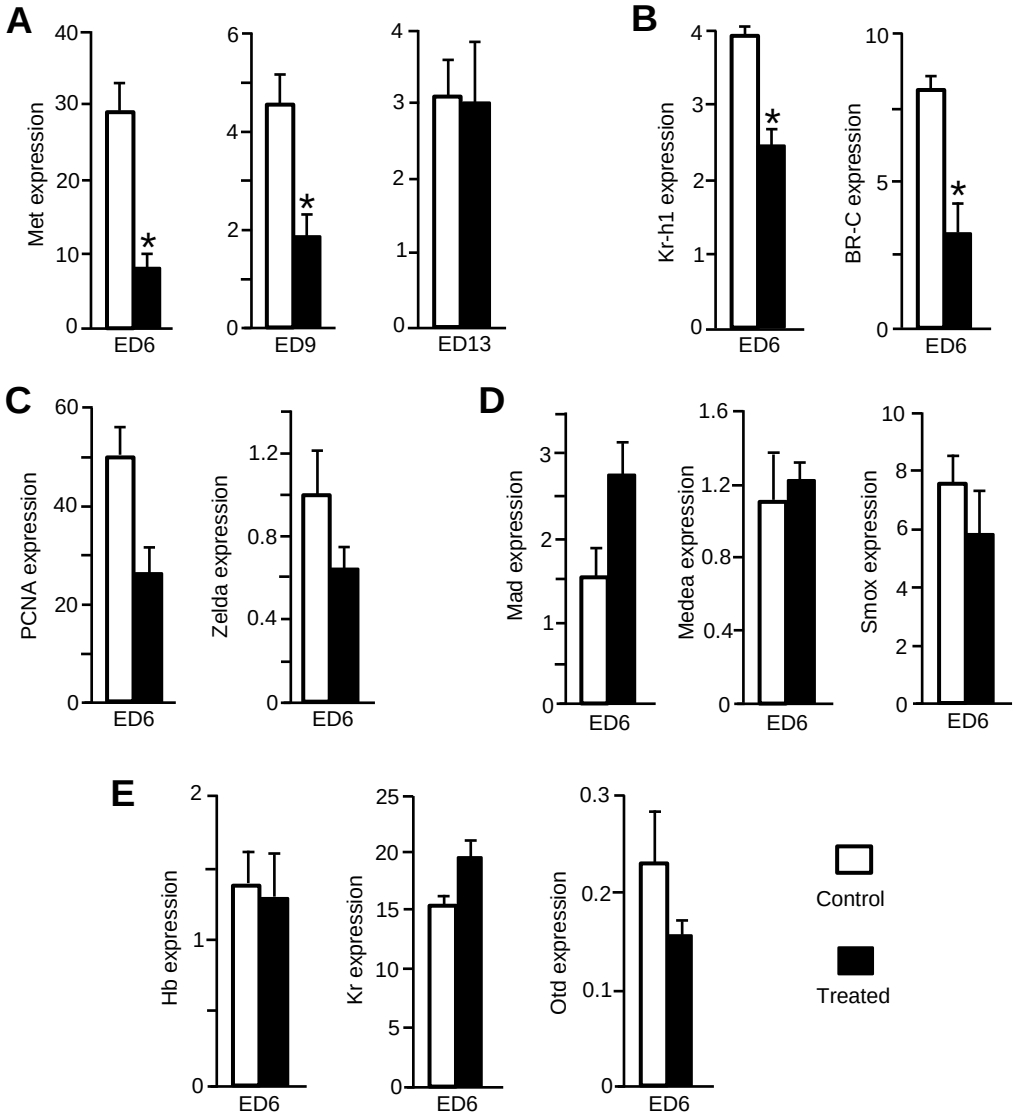

Fig. S2. Effects of maternal RNAi of Met in embryos of *Blattella germanica*. (A) Met mRNA levels; dsMet (or dsMock, in controls) was administered on 5-day-old adult females, and measurements were carried out on ED6, ED9 and ED13. (B) Effects on the expression of Kr-h1 and BR-C, measured on ED6, when Met transcripts are more effectively depleted. (C) Expression of PCNA and Zelda on ED6. (D) Expression of the Smads of the TGF-β pathways, Mad, Medea and Smox on ED6. (E) Expression of gap genes Hunchback (Hb), Krüppel (Kr) and Orthodenticle (Otd) on ED6. Each measurement represents three biological replicates and results of qRT-PCR are expressed as copies of the examined transcript per 1000 copies of BgActin-5c mRNA. Data are represented as the mean ± SEM. The asterisk indicates statistically significant differences with respect to controls ($p < 0.05$), calculated on the basis of the REST (Pfaffl et al., 2002).

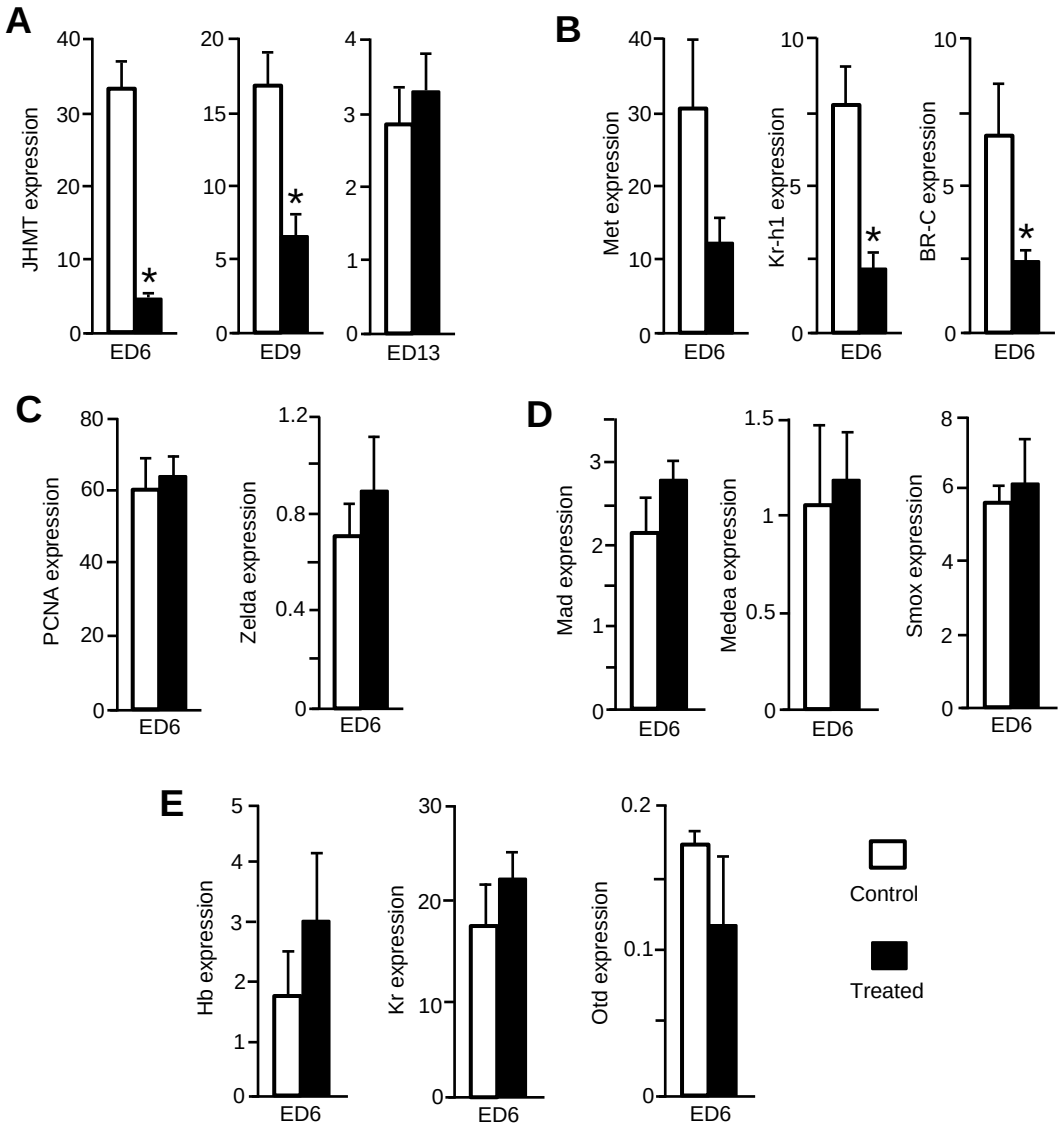

Fig. S3. Effects of maternal RNAi of JHAMT in embryos of *Blattella germanica*. (A) JHAMT mRNA levels; dsJHAMT (or dsMock, in controls) was administered on 5-day-old adult females, and measurements were carried out on ED6, ED9 and ED13. (B) Effects on the expression of Met, Kr-h1 and BR-C, measured on ED6, when JHAMT transcripts are more effectively depleted. (C) Expression of PCNA and Zelda on ED6. (D) Expression of the Smads of the TGF-β pathways, Mad, Medea and Smox on ED6. (E) Expression of gap genes Hunchback (Hb), Krüppel (Kr) and Orthodenticle (Otd) on ED6. Each measurement represents three biological replicates and results of qRT-PCR are expressed as copies of the examined transcript per 1000 copies of BgActin-5c mRNA. Data are represented as the mean ± SEM. The asterisk indicates statistically significant differences with respect to controls ($p < 0.05$), calculated on the basis of the REST (Pfaffl et al., 2002).

Table S1. Summary of the effects of maternal RNAi of JHMT, Met or Kr-h1 on ootheca fate. Otheca was formed on day 8 of adult life in treated and controls, that is 3 days after the dsRNA injection. In controls, all oothecae eclosed on day 18 after their formation (see main text).

Factor targeted	n	Oothecae dropped between days 2 and 3	Oothecae dropped between days 7 and 16	Oothecae transported beyond day 19	Othecae that eclosed on day 18
JHAMT	68	8 (11.8%)	0	12 (17.6%)	48 (70.6%)
Met	45	0	0	5 (11.1%)	40 (88.9%)
Kr-h1	70	12 (17.1%)	5 (7.1%)	23 (32.9%)	30 (42.9%)

Table S2. Summary of the phenotypes observed in not hatched oothecae from females treated with dsRNA targeting JHMT, Met or Kr-h1, examined on day 19. In controls, all oothecae eclosed on day 18 (see main text).

Factor targeted	Oothecae	Embryos examined	Phenotype A	Phenotype B	Phenotype C	Phenotype D
JHAMT	8	195	114 (58.5%)	44 (22.6%)	3 (1.5%)	34 (17.4%)
Met	5	190	47 (24.7%)	65 (34.2%)	53 (27.9%)	25 (13.2%)
Kr-h1	18	452	176 (38.9%)	102 (22.6%)	79 (17.5%)	95 (21%)

Table S3. Primers used for transcript measurements and to prepare dsRNAs. In the Primer name, "RT" indicated that the pair was used for transcript measurements and "RNAi" to prepare dsRNAs. In the Primer sequence, "F" means forward, and "R" reverse.

Gene name	Accession number	Primer name	Primer sequence	Amplicon length (bp)
Actin 5c	EMBL: AJ862721	BgActin-5c	F: 5'-AGCTTCCTGATGGTCAGGTGA-3' R: 5'-ACCATGTACCCTGGAATTGCCGACA-3'	213
A. californica nucleopoydrovirus	EMBL: K01149	BgMock-RNAi	F: 5'-ATCCTTTCCTGGGACCCGGCA-3' R: 5'-ATGAAGGCTCGACGATCCTA-3'	307
Broad Complex (BR-C) (core)	EMBL: FN651774	BgBrCore-RT	F: 5'-CGGGTCGAAGGGAAAGACA-3' R: 5'-CTTGGCGCCGAATGCTGCGAT-3'	76
Bursicon	EMBL: LN901328	BgBurs-RT	F: 5'-AATGGACGAGTGTCAGGTGACA-3' R: 5'-ATGGAACGTTCATGCATGTGTT-3'	158
Connectin	EMBL: LT717637	BgCon-RT	F: 5'-GGCTGCCAGAGTTGAGAAAG-3' R: 5'-GAAGAGCTGGAGTTGAACGG-3'	106
Hunchback (Hb)	EMBL: LT717629	BgHb-RT	F: 5'-TCTAAATTGCCCACCAGGTC-3' R: 5'-CCATGAGTTGGAGCCTGAAT-3'	120
Integrin Beta	EMBL: LT717638	BgITGB-RT	F: 5'-GCGAGTTTTCTGGAGAGGTG-3' R: 5'-CCATTATGCAAGCTGTGGTG-3'	92
Juvenile Hormone Acid Methyltransferase (JHAMT)	EMBL: LT716988	BgJHMT-RT	F: 5'-GACCTGGTGGTGAAGTCTTGG-3' R: 5'-TGACTCCATTTCGATTTTTTACTCTG-3'	91
Juvenile Hormone Acid Methyltransferase (JHAMT)	EMBL: LT716988	BgJHMT-RNAi	F: 5'-CTTCTGTCTGCATTTTGTAGTGGAT-3' R: 5'-TGGCTTGTAGTGAATCTTGAAGAA-3'	325
Kettin	EMBL: LT717636	BgKettin-RT	F: 5'-GAATGGCAGCAGTCAGTGAA-3' R: 5'-GAAACAAGGCTTCGTGAAGC-3'	104
Krüppel (Kr)	EMBL: LT717630	BgKr-RT	F: 5'-CGTACACACACGGGAGAAAA -3' R: 5'-ATTGTGACCGGCAATTTGTT -3'	84
Krüppel- homolog 1 (Kr-h1)	EMBL: HE575250	BgKr-h1-RT	F: 5'-GCGAGTATTGCAGCAAATCA-3' R: 5'-GGGACGTTCTTTCGTATGGA-3'	77
Krüppel- homolog 1 (Kr-h1)	EMBL: HE575250	BgKr-h1-RNAi	F: 5'-GAATCTCAGTGTGCATAGGCG-3' R: 5'-CCTTGCCACAAATGACACAA-3'	320
Laccase 2	EMBL: LT717634	BgLaccase2-RT	F: 5'-TGGTGAATGTGGAACCAAGA-3' R: 5'-TACGATGTTGGTCTCCCACA-3'	108
Medea	EMBL: LN901332	BgMed-RT	F: 5'-AGGTGTGGTGGGAGGTACTG-3' R: 5'-TTGTTTGAGGAACCGTGTGA-3'	71
Methoprene-Tolerant (Met)	EMBL: HG965209	BgMet-RT	F: 5'-CTGTTGGGACATCAGCAGAA-3' R: 5'-GGCAGGTGATGGAGTGAAGT-3'	58
Methoprene-Tolerant (Met)	EMBL: HG965209	BgMet-RNAi	F: 5'-GCAAATTGTATCCTTCATCTGC-3' R: 5'-TGACAGACTCGCGCTTTATG-3'	458
Mothers against dpp (Mad)	EMBL: LN901331	BgMad-RT	F: 5'-TCAACAGCCTTTTCTGCCCA-3' R: 5'-TGGATGCTGATGAAGCGGAA-3'	148
Myosin Heavy Chain (MHC)	EMBL: LT717632	BgMHC-RT	F: 5'-ACACCAGGAAGAACCACCAG-3' R: 5'-CTGAGTGCCTCAGCCTTACC-3'	85
Orthodenticle (Otd)	EMBL: LT717631	BgOtd-RT	F: 5'- GACGCGGTATCCTGACATCT-3' R: 5'- GCTGTTTTTGCTGTTGACGA-3'	122
Proliferating cell nuclear antigen (PCNA)	EMBL: LT717627	BgPCNA-RT	F: 5'-GAAGCTGGCACAGACAACAA-3' R: 5'-GGCCTTGGTGAAAGAATTGA-3'	124
Smad on X (Smox)	EMBL: LT575495	BgSmox-RT	F: 5'-GACACATTGGGAAAGGCGTT-3' R: 5'-GACTGTGATAAGAGCGCTGC-3'	202
Trio	EMBL: LT717633	BgTrio-RT	F: 5'- AGTCTTGAAGCCTTGCCAAA -3' R: 5'-CTGCTGCTTGCCATACAAAA -3'	130
Zelda	EMBL: LT717628	BgZld-RT	F: 5'- TGTCCCAAACAGTTCAACCA-3' R: 5'-AAAGGGTTTCTCTCCCGTGT-3'	72